J. Biochem. **138**, 553–562 (2005)
doi:10.1093/jb/mvi154

26 kDa Endochitinase from Barley Seeds: An Interaction of the Ionizable Side Chains Essential for Catalysis

Tsuneo Ohnishi[1], André H. Juffer[2], Masahiro Tamoi[1], Karen Skriver[3] and Tamo Fukamizo[1,*]

[1]Department of Advanced Bioscience, Kinki University, 3327–204 Nakamachi, Nara, 631-8505; [2]Biocenter and Department of Biochemistry, University of Oulu, FIN-90014 Oulu, Finland; and [3]Institute of Molecular Biology, University of Copenhagen, 2A Øster Farimagsgade, 1353 Copenhagen K, Denmark

Received June 7, 2005; accepted July 31, 2005

To explore the structure essential for the catalysis in 26 kDa endochitinase from barley seeds, we calculated theoretical pK_a values of the ionizable groups based on the crystal structure, and then the roles of ionizable side chains located near the catalytic residue were examined by site-directed mutagenesis. The pK_a value calculated for Arg215, which is located at the bottom of the catalytic cleft, is abnormally high (>20.0), indicating that the guanidyl group may interact strongly with nearby charges. No enzymatic activity was found in the Arg215-mutated chitinase (R215A) produced by the *Escherichia coli* expression system. The transition temperature of thermal unfolding (T_m) of R215A was lower than that of the wild type protein by about 6.2°C. In the crystal structure, the Arg215 side chain is in close proximity to the Glu203 side chain, whose theoretical pK_a value was found to be abnormally low (–2.4), suggesting that these side chains may interact with each other. Mutation of Glu203 to alanine (E203A) completely eliminated the enzymatic activity and impaired the thermal stability (ΔT_m = 6.4°C) of the enzyme. Substrate binding ability was also affected by the Glu203 mutation. These data clearly demonstrate that the Arg215 side chain interacts with the Glu203 side chain to stabilize the conformation of the catalytic cleft. A similar interaction network was previously found in chitosanase from *Streptomyces* sp. N174 [Fukamizo *et al.* (2000) *J. Biol. Chem.* 275, 25633–25640]; hence, this type of interaction seems to be at least partly conserved in the catalytic cleft of other glycosyl hydrolases.

Key words: catalytic cleft, chitinase, site-directed mutagenesis, theoretical pK_a calculation, thermal unfolding.

Abbreviations: GlcNAc, 2-acetamido-2-deoxy-D-glucopyranose; $(GlcNAc)_n$, β-1,4–linked oligosaccharide of GlcNAc with a polymerization degree of *n*; SDS-PAGE, sodium dodecyl sulfate–polyacrylamide gel electrophoresis; CD, circular dichroism.

The catalytic reactions of glycosyl hydrolases have been recognized to take place through the concerted action of two carboxyl side chains of acidic amino acid residues. One of the two carboxylates donates its proton to glycosyl oxygen, and the other stabilizes the transition state of the hydrolytic reaction or activates the water molecule, which attacks the C1-carbon of the substrate sugar residue. The carboxylate acting as the proton donor is usually in a specific environment that is favorable to efficient proton donation. In hen egg white lysozyme, the catalytic residue Glu35 is in a hydrophobic environment that results from its close proximity to Trp108 (*1*). The hydrophobic effect is supposed to elevate the pK_a value of Glu35, enabling efficient proton donation, even in the higher pH region (5 to 6). Two tryptophan residues appear to create a similar hydrophobic environment for the catalytic residue of an endoglucanase from *Bacillus* sp. (*2*). In our previous paper, we reported that the interaction network of ionizable side chains is essential for the catalytic activity of chitosanase from *Streptomyces* sp. N174 (*3*). This interaction network consists of the Arg205, Asp145, and Arg190 side chains, and appears to create a specific environment favorable to proton donation of the catalytic residue, Glu22. On the other hand, the *Streptomyces* chitosanase and 26 kDa endochitinase from barley seeds have been reported to have an invariant catalytic core consisting of two α-helices and a three-stranded β-sheet (*4*). Such an invariant fold of the catalytic cleft causes various similarities in structure and function between these enzymes (*5*). This prompted us to presuppose a similar interaction network consisting of ionizable side chains in the catalytic cleft of the barley chitinase.

The 26 kDa endochitinase from barley seeds belongs to family GH19 (*6*), and its three-dimensional structure has been solved by X-ray crystallography (*7*). As shown in Fig. 1, the enzyme is composed of two lobes, each of which is rich in α-helical structure, and the substrate binding cleft lies between the two lobes. A site-directed mutagenesis study revealed that Glu67 and Glu89 are essential for its catalytic activity (*8*). Because of the anomer inversion in the hydrolytic products of the barley chitinase reaction (*9*, *10*), the catalytic reaction is supposed to take place through a single displacement mechanism; that is, immediately after the proton-donation from Glu67 to the glycosyl oxygen, a water

*To whom correspondence should be addressed. Tel: +81-742-43-8237, Fax: +81-742-43-8976, E-mail: fukamizo@nara.kindai.ac.jp

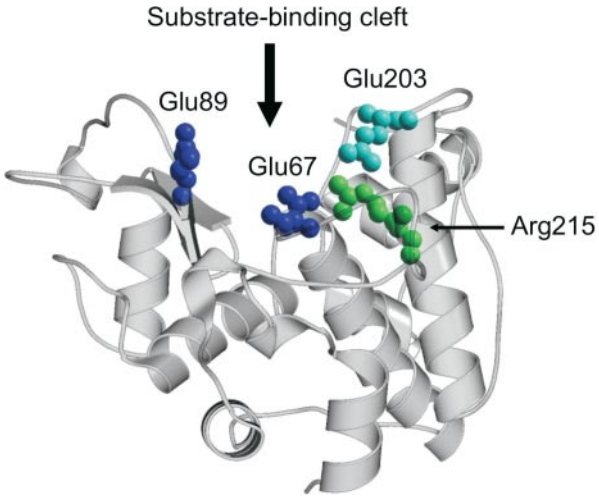

Fig. 1. **X-ray crystal structure of chitinase from barley seeds.** The structure was created using the coordinate file, PDB entry 2baa (Hart *et al.*, 1995). The catalytic residues (Glu67 and Glu89) and the mutated residues in this study (Arg215 and Glu203) are highlighted in the space-filling model.

molecule activated by the Glu89 carboxylate is believed to attack the C1-carbon of the substrate sugar residue from the α-side. However, the mechanistic details of the catalytic reaction of enzymes belonging to family GH19 remain unclear, whereas the enzyme mechanism of chitinases belonging to family GH18 has been more clearly elucidated by X-ray crystallographic studies by several investigators (*11–13*). To examine the mechanistic details of the catalytic reaction, it is essential to gain an insight into the microenvironment surrounding the catalytic carboxylate. Our previous study on the *Streptomyces* chitosanase demonstrated that the theoretical pK_a calculation made according to the method of Juffer *et al.* (*14*) is useful for examining the states of the ionizable side chains of proteins. This is because the interactions of ionizable side chains markedly shift their pK_a values from those of free compounds of the corresponding amino acids. The pK_a calculation provides important information on the microenvironment surrounding the catalytic residue.

In this study, we have paid attention to some of the ionizable amino acid residues near the catalytic residue Glu67 of the barley chitinase, and calculated the theoretical pK_a values of the ionizable amino acids of the enzyme protein. Based on the calculated results, Arg215 and Glu203 are believed to be important for the catalytic activity of the chitinase. Then, site-specific mutations of these two residues were conducted, and the mutated enzymes (R215A and E203A) were subjected to activity and stability measurements.

MATERIALS AND METHODS

Materials—Oligonucleotide primers for PCR and sequencing were purchased from SAWADY Co. All reagents for *Escherichia coli* cultivation and enzyme production were purchased from Wako Pure Chemical Co. and Nakalai Tesque Co. Restriction enzymes for gene manipulations were from TOYOBO and Nippon Gene Co. Macro-Prep CM Support and Bio-Gel A-0.5 m used for enzyme purification were the products of Bio-Rad Lab. The glycol chitin used for the enzyme assay was prepared by the method of Yamada and Imoto (*15*). *N*-Acetylglucosamine oligosaccharides [$(GlcNAc)_n$ n = 2, 3, 4, 5, and 6] were purchased from Seikagaku Kogyo Co. Other reagents were of analytical grade commercially available.

Theoretical pK_a Calculation—The prediction of the acid dissociation constants (pK_a) of the barley chitinase was performed for the protein structure in entry 2baa (*7*) from the Protein Databank (*16*). The method to calculate pK_a has been described in full detail elsewhere (*3*, *14*). In brief, the calculation consists of two main steps.

First, the intrinsic pK_a is calculated. This pK_a corresponds to the pK_a for which the interaction between different titrating sites in the protein are ignored. Interactions are of an electrostatic nature only and are computed by applying continuum electrostatics and the boundary element method (*17*). This method solves a pair of integral equations on the dielectric boundary that encloses the protein and separates the solvent from the protein. The boundary ensures that mutual polarization effects due to differences in the dielectric properties of the protein and the solvent are included, as is manifest in the different dielectric constants. The dielectric constant of the protein was set to 20.0, while the dielectric constant of the solvent was 78.5. The higher dielectric constant value for the protein (20.0) was found to be the most appropriate to approximately correct for the conformational flexibility, which is ignored in the calculation procedure, and to attain consistency between the experimental and calculated pK_a values for various proteins (*14*). The intrinsic pK_a is computed from the shift in the given pK_a of the titrating site in the model compound (free residue) when it is transferred from the solvent into the protein location. The solvent is an electrolyte (NaCl) with a given ionic strength. In this work, the ionic strength was set to 0.15 M.

The second step of the calculation computes an additional shift in the pK_a due to the interactions between the titrating sites. For this, the accessible protonation states of the protein as a function of pH are sampled. This is accomplished with a Monte Carlo simulation that probes different distributions of protons over the available titrating sites. In this way, a titration curve (the average proton occupancy as a function of pH) of each individual site (and also of the full protein) is obtained, so that the apparent pK_a of each site is determined.

The finite difference method has been more commonly employed for the calculation of the electrostatic potential, because of its higher computational efficiency (*18*). The boundary element method employed in this study, however, has recently been validated against experimental data using lysozyme, acid phosphatase, protein disulfide isomerase, and calbindin, and shown to be a much more accurate method (*14*, *19–21*). One reason is that the direct Coulomb interaction is calculated in an exact manner without any approximations, so that any numerical error solely arises from the reaction field terms. This method tends to be more sensitive to the exact details of the protein structure.

Enzyme Production and Purification—The *E. coli* expression vector of the barley chitinase reported previously (*8*) was transformed into *E. coli* Origami(DE3)pLysS, which

was then grown to A_{600} = 0.6 at 37°C before induction with 0.1 mM isopropyl β-D-thiogalactopyranoside (IPTG). After induction, growth was allowed to continue for 3 h at 37°C with shaking at 140 rpm. Cells were harvested by centrifugation at 5,000 rpm for 10 min at 4°C, and then lysed by sonication according to the method previously reported (*8*). Insoluble materials were removed by centrifugation at 15,000 rpm for 10 min at 4°C, and the soluble fraction was dialyzed against 5 mM sodium phosphate buffer containing 10 mM NaCl (pH 7.0). Then, the dialyzed fraction was applied onto a cation exchange column of Macro-Prep CM Support (18 × 70 mm) equilibrated with the same buffer. After elution with the phosphate buffer, the chitinase fraction was eluted with a linear gradient elution of NaCl (from 10 to 200 mM). The chitinase active fractions were pooled and dialyzed against 50 mM sodium phosphate buffer at pH 7.0, applied to a gel filtration column of Bio-Gel A-0.5 m, and then eluted with the same buffer. The chitinase preparation purified by gel-filtration was stored at 4°C, and used for subsequent experiments.

Site-Directed Mutagenesis—The expression plasmid was denatured, and annealed with the mutagenic primer listed below. *PfuTurbo* DNA polymerase was used for the extension of the mutated circular strand. After digestion of the nonmutated parental DNA template by *Dpn*I, the mutated double-stranded DNA was transformed into *E. coli* DH-5α competent cells to repair the nicks in the mutated plasmid. The resulting mutated plasmids were used for the production of mutated chitinases. The mutagenic primers used were 5′-AGCCGCGTCGCCGATGCAATCGGGTTTTAC-3′ (antisense) and 5′-GTAAAACCCGATTGCATCGGCGACG-CGGCT-3′ (sense) for the production of R215A, and 5′-CC-GTGACCGCACGCGATCCCGCCGTTGATG-3′ (antisense) and 5′-CATCAACGGCGGGATCGCGTGCGGTCACGG-3′ (sense) for E203A. Glu67-mutated chitinase (E67Q) was produced according to the method previously reported (*8*).

Enzyme Assay—Chitinase activity was determined using glycol chitin as the substrate. A reaction mixture containing 0.2 ml of 0.3% glycol chitin, 0.4 ml of 0.1 M Tris-HCl buffer (pH 7.0), and 0.2 ml of enzyme solution was incubated for 15 min at 37°C. The reducing sugar generated by the degradation of the substrate was measured using a modified Schales' procedure (*22*). To ensure the enzymatic activity thus determined, *N*-acetylglucosamine hexasaccharide was hydrolyzed by the enzymes, and the reaction products were analyzed by gel-filtration HPLC using a column of TSK-GEL G2000PW (Tosoh) eluted with distilled water at a flow rate of 0.3 ml/min.

Protein Concentration—Protein concentrations were determined from their ultraviolet absorption at 280 nm using the extinction coefficients calculated from the equation reported by Pace *et al*. (*23*).

Electrophoresis of the Protein—SDS–polyacrylamide gel electrophoresis was performed according to the method of Laemmli (*24*) using the molecular weight marker "Daiichi" II (Daiichi Pure Chemicals) as a standard. Protein bands were detected by staining with Coomassie Brilliant Blue R-250.

Circular Dichroism (CD)—The chitinase preparations were dialyzed against 50 mM sodium phosphate buffer, pH 7.0. The CD spectra were recorded using a Jasco J-720 spectropolarimeter (cell length, 0.1 cm).

Thermal Unfolding—To obtain the thermal unfolding curve of the enzyme protein, the CD value at 222 nm was monitored by raising the solution temperature at a rate of 1°C/min. Setting the thermocouple in the cell, the solution temperature was directly measured by a model DP-500 (Rikagaku Kogyo). To facilitate comparisons between the unfolding curves obtained, the experimental data were normalized as follows. Fractions of unfolded protein at individual temperatures were calculated from the CD value by linearly extrapolating the pre- and post-transition baselines into the transition zone, and plotted against the temperature. Assays were performed in duplicate. Thermodynamic parameters could not be obtained because of the poor reversibility of the unfolding transition. When the unfolding experiments were conducted in the presence of the ligands, $(GlcNAc)_n$ (n = 3 and 6), the unfolding process was monitored by the tryptophan fluorescence intensity obtained from excitation at 295 nm UV light using a Hitachi F-3010 spectrofluorometer.

RESULTS AND DISCUSSION

Theoretical Calculation of pK_a Values—Theoretical pK_a values of the ionizable side chains of 26 kDa endochitinase from barley seeds were deduced using the method of Juffer *et al*. (*14*). The calculation was successful as in the case of *Streptomyces* sp. N174 chitosanase (*3*). The pK_a values calculated are listed in Table 1. The value for Arg215 is

Table 1. **Calculated pK_a values of the ionizable side chains of the barley chitinase.**

Amino acid residue	pK_a value	Amino acid residue	pK_a value
N-term (1)	7.5	His 121	5.8
Arg 8	14.6	Tyr 123	10.1
Asp 12	2.1	Tyr 125	10.4
Arg 13	13.5	Arg 130	12.3
His 17	10.0	Asp 135	3.1
Arg 18	17.3	Asp 141	1.5
Asp 20	0.8	Asp 146	3.0
Lys 26	10.9	Lys 152	11.7
Tyr 29	14.8	Lys 165	12.9
Tyr 31	11.1	His 169	7.9
Asp 32	1.2	Asp 182	1.9
Asp 51	4.0	Arg 183	12.6
Lys 54	13.5	Arg 187	14.6
Arg 55	15.9	Glu 203	–2.4
Glu 56	2.2	His 206	8.4
His 66	8.0	Asp 209	0.2
Glu 67	1.8	Arg 211	15.6
Asp 77	2.5	Asp 214	1.6
Tyr 84	15.2	Arg 215	23.5
Lys 87	12.1	Tyr 219	13.6
Glu 89	4.3	Lys 220	12.9
Arg 90	12.4	Arg 221	17.1
Asp 95	3.0	Tyr 222	10.6
Tyr 96	13.3	Asp 224	4.4
Lys 109	12.6	Tyr 230	13.0
Arg 110	14.8	Asp 235	3.2
Tyr 111	10.9	Tyr 237	11.1
Tyr 112	9.2	Arg 240	13.0
Arg 114	22.3	C-term (243)	3.2

greater than 20.0, a result usually indicating that the side chain is involved in a strong interaction with nearby charges (*14*, *18*). In the crystal structure, Arg215 is in close proximity to Glu203 (Fig. 1), which has the calculated pK_a value of –2.4. The large shifts in the pK_a values observed for the Arg215 and Glu203 side chains suggest that Arg215 might interact strongly with Glu203.

In hen egg white lysozyme, an abnormal pK_a value of 6.3 was obtained experimentally obtained for Glu35, which acts as the proton donor (*1*, *25*). The higher pK_a value is regarded as an important factor for retaining activity over a wide pH range, and is supposed to be derived from the close proximity of the hydrophobic side chain of Trp108. In the previous paper on the barley chitinase (*9*), the pK_a value of Glu67 was reported to be 6.8 based on the pH-activity profile. Since the apparent pK_a value predicted from the pH-activity profile is generally regarded as that of the unbound enzyme protein (*26*), the pK_a value calculated based on the free enzyme structure should be consistent with the apparent pK_a value from the pH-activity profile. However, the theoretical pK_a value of the proton donor carboxylate (Glu67) was calculated to be 1.8, which is much lower than the apparent pK_a value (6.8). The discrepancy between the calculated and apparent pK_a values of Glu67 might be due to a specific and complicated environment of the glutamic acid, which could not be modeled in the usual calculation procedures. The complications of the electrostatic environment of Glu67 might be associated with conformational flexibility or relaxation upon changes in the ionization state of the enzyme protein.

Several other amino acids in Table 1 also exhibit abnormal pK_a values; for example, the value for Arg114 is also abnormally high (>20.0), indicating that Arg114 interacts with a nearby charge, probably Glu89, the second carboxylate essential for catalysis (*8*). In this study, however, we decided to focus our attention on Arg215 and Glu203, which are located very close to Glu67 and are considered to interact most strongly with each other.

Production of Mutated Chitinases (R215A and E203A)—The amount of soluble wild type enzyme produced by our expression system was reported to be 15 mg/liter (*8*). A comparable amount of E203A could be produced in the soluble fraction, whereas for R215A the maximum yield of the soluble material was only 10% that of the wild type. Protein folding appears to be suppressed in this mutant enzyme. By repeated cultivation of the *E. coli* strain harboring the R215A gene, we finally obtained a sufficient amount of the mutant enzyme in a soluble state. After the two step purification, all chitinases were obtained in sufficient purity. The SDS-PAGE profiles of these enzymes are shown in Fig. 2.

Enzymatic Activity of R215A—To examine the role of Arg215 in chitinase catalysis, we measured the hydrolytic activity of R215A. At first, the enzymatic activity was examined using glycol chitin as the substrate. The mutant chitinase did not show any enzyme activity. When *N*-acetylglucosamine hexasaccharide was used instead of glycol chitin, the wild type enzyme produced dimers, trimers, and tetramers as shown in the left panel of Figure 3. However, R215A did not produce any oligosaccharide product (Fig. 3, right panel). The Arg215 mutation was found to completely eliminate the enzymatic activity.

Structure and Thermal Stability of R215A—CD spectra of the wild type and mutated chitinases are shown in Fig. 4.

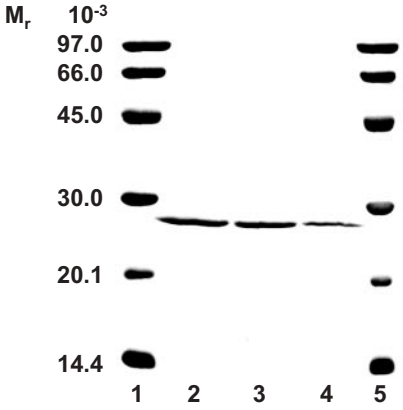

Fig. 2. **SDS-PAGE of the purified wild type and mutated chitinases (R215A and E203A).** Lanes 1 and 5, molecular size markers; Lane 2, wild type; Lane 3, E203A; Lane 4, R215A.

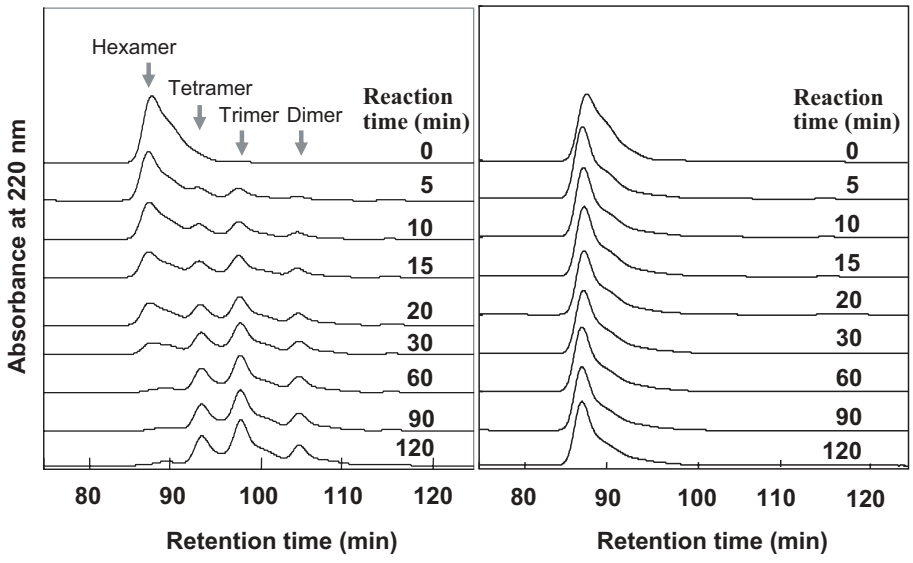

Fig. 3. **HPLC profiles showing the enzymatic hydrolysis of *N*-acetylglucosamine hexasaccharide.** The enzymatic reaction was conducted in 50 mM sodium acetate buffer, pH 5.0, at 40°C. Left panel, wild type; Right panel, R215A.

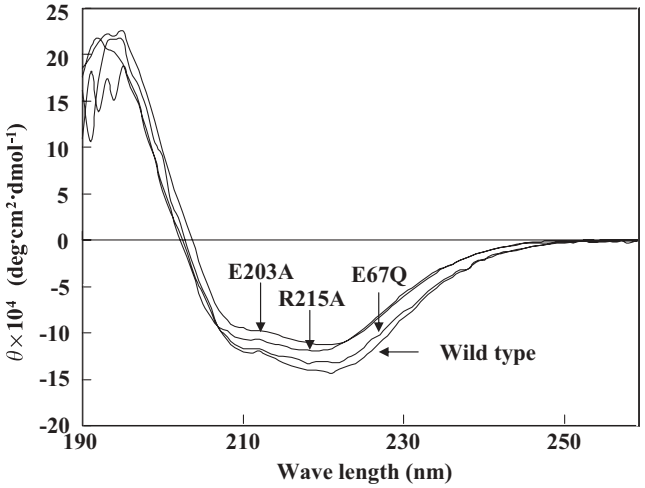

Fig. 4. **CD spectra of the wild type, E67Q, R215A and E203A.** The spectra were recorded in 50 mM sodium phosphate buffer, pH 7.0, at 20°C.

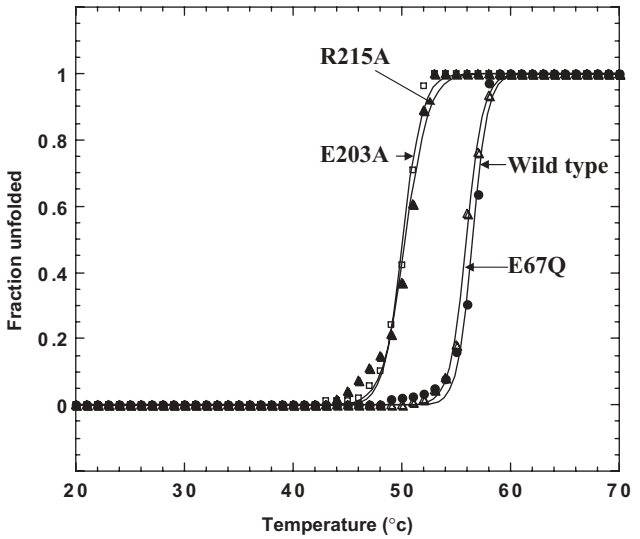

Fig. 5. **Thermal unfolding curves of wild type, E67Q, R215A and E203A.** The unfolding transitions were monitored by the CD value at 222 nm in 50 mM sodium acetate buffer at pH 7.0. Solid circles, wild type; open triangles, E67Q; open squares, E203A; and solid triangles, R215A. The transition temperatures calculated from the transition curves are listed in Table 2.

The negative CD value derived from the α-helices of the enzyme protein was found to be somewhat suppressed in R215A as compared with that of the wild type, indicating that the secondary structure is partly unfolded by the Arg215 mutation. The thermal unfolding curve obtained by monitoring CD at 222 nm is shown in Fig. 5. From the unfolding curves, the transition temperature of thermal unfolding (T_m) was calculated to be 56.5°C for the wild type and 50.3°C for R215A (ΔT_m = 6.2°C). The Arg215 mutation had a considerable effect on the thermal stability, suggesting that the Arg215 side chain might possibly interact with nearby charges, and that the interaction might be essential for the catalytic activity.

Table 2. **The transition temperatures of thermal unfolding transitions (T_m) of the wild type barley chitinase and its mutants, R215A and E203A.**

Enzyme	T_m (°C)	
	CD at 222 nm	Fluorescence at 320 or 340 nm (excitation at 295 nm)
Wild type	56.5	
E67Q	55.9	53.9
+$(GlcNAc)_3$		57.7
+$(GlcNAc)_6$		56.6
R215A	50.3	
E203A	50.1	48.2
+$(GlcNAc)_3$		47.8
+$(GlcNAc)_6$		47.6

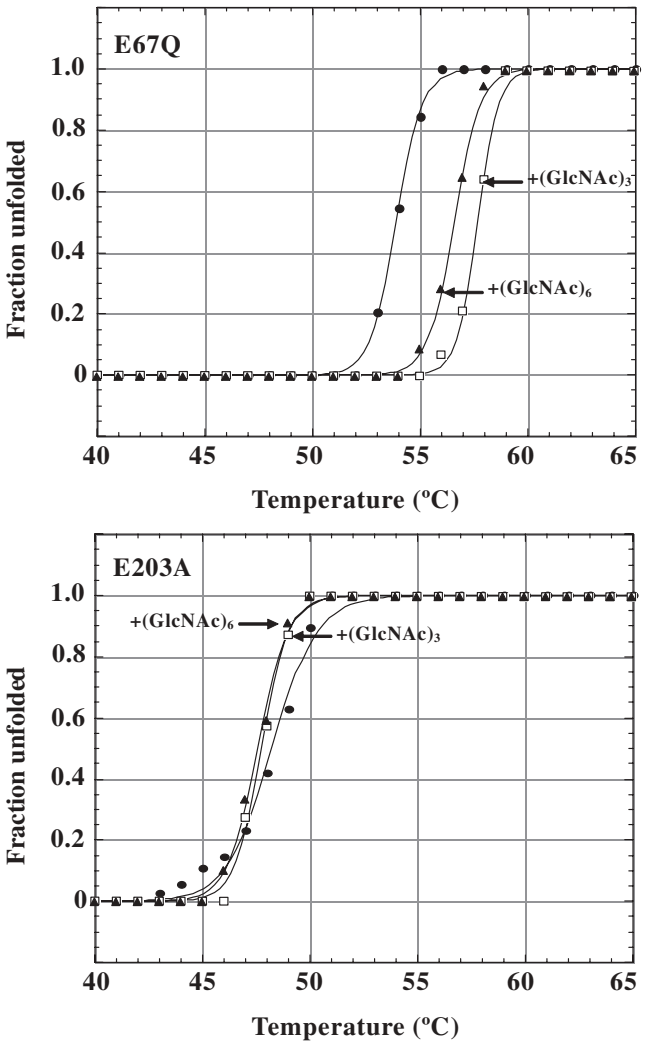

Fig. 6. **Thermal unfolding curves of E67Q and E203A in the presence of oligosaccharide ligands, $(GlcNAc)_3$ and $(GlcNAc)_6$.** The unfolding transitions were conducted with 50 mM sodium acetate buffer at pH 7.0, and monitored by their tryptophan fluorescence intensity at 320 nm for E67Q and at 340 nm for E203A. solid circles, without ligand; open squares, in the presence of $(GlcNAc)_3$; solid triangles, in the presence of $(GlcNAc)_6$. The transition temperatures calculated from the transition curves are listed in Table 2.

Enzymatic Activity of E203A—As described above, the Glu203 side chain was found to be close to the Arg215 side chain (Fig. 1), and its pK_a value was calculated to be –2.4 (Table 1). Glu203 is the more probable candidate for the counterpart of the Arg215 interaction. Thus, we produced E203A, and measured its enzymatic activity. As in the case of R215A, the E203A mutant did not show any enzyme activity toward glycol chitin or *N*-acetylglucosamine hexasaccharide (data not shown). The enzymatic activity was completely abolished by the Glu203 mutation.

Structure and Thermal Stability of E203A—As shown in Fig. 4, the Glu203 mutation was found to affect the negative CD value derived from the α-helices in a manner similar to the Arg215 mutation. The T_m value calculated from the thermal unfolding curve of E203A shown in Fig. 5 was 50.1°C. The ΔT_m induced by the Glu203 mutation was 6.4°C. The effect of the Glu203 mutation on the thermal stability is very similar to that of the R215 mutation.

Comparison with the Chitinase Possessing Mutation at the Catalytic Residue Glu67—Andersen *et al*. (*8*) studied the mutant enzyme, in which the catalytic residue Glu67 is substituted with glutamine (E67Q). E67Q has been reported to be completely inactive, and the CD spectrum of E67Q indicated that the secondary structure is retained after the Glu67 mutation. In this study, we reexamined the activity and CD spectrum of E67Q, and then measured the thermal unfolding curve of the mutant enzyme to compare it with those of R215A and E203A. E67Q did not produce any oligosaccharide product from the hexasaccharide substrate (data not shown), whereas its CD spectrum was almost identical to that of the wild type, as shown in Fig. 4. The T_m value of E67Q (55.9°C) was also similar to that of the wild type; hence, the thermal stability was not affected by the Glu67 mutation (Fig. 5). The T_m values obtained are summarized in Table 2.

As described above, the pK_a value of Glu67 estimated from the experimental pH-activity profile is considerably higher (6.8) than that of free glutamic acid (*9*). Thus, the Glu67–Arg215 interaction is unlikely to occur, because the basic group would rather lower the carboxylate pK_a. The effect of the Glu67 mutation on the thermal stability of the enzyme protein is not consistent with that of the Arg215 mutation, suggesting also that the Glu67–Arg215 interaction is unlikely. However, the Arg215 mutation affected the thermal stability in a manner similar to that of the Glu203 mutation, suggesting that the Arg215 side chain really interacts with Glu203. The abnormal values of

```
barley       192 GVITNIINGG IECGHG-QDS RVADRIGFYK RYCDILGVGY 230
garlic1      247 GVITNIINGG VECGHGS-DT HVADRIGYYK RYCDLLQVGY 285
garlic2      236 GVITNIINGG VECGHGS-DP SVADRIGFYK RYCDLFQVGY 274
kidney bean  237 GTVTNIINGG LECGRG-QDS RUQDRIGFFK RYCDLLGVGY 275
yam          206 GATIRIINGG QEC-DGHNTA QMMARVGYYQ EYCAQLGVSP 244
brassica     202 GATIRAING- MEC-NGGNSG AVNARIRYYR DYCGQLGVDP 239
poppulus1    153 GVITNIINGG IECGQGGPNA ANEDRIGFYK KYCDSLGTTY 192
populaus2    255 GMLTNIITNG GECTKDGK-T RQQNRIDYYL RYCDMLQVDP 293
zea may1     267 GVVTNISNGG LECGHGA-DS RVADRIGFYK RYCDLLGVSY 305
zea may2     213 GVITNIING- IECGKGYNE- KVANRTFFYT SYCDILGISY 250
RSC-a        251 GVITNIVNGG IECGHGQ-DS RVADRIGFYK RYCDILGVGY 289
Oschia1a     271 GVVTNIINGG VECGHGA-DS RVADRIGFYK RYCDMLGVSY 309
Petunia      201 GVITNIINGG IECGKG-QNA RVEDRIGYYR RNVSIMNVAP 239
RSC-c        192 GVITNIINGG LECGHGQ-DS RVADRIGFYK RYCDILGVGY 230
Oschia2a     210 GVITNIINGG IECGVG-QND ANVDRIGYYK RYCDMLGAGY 248
D.oppo4      234 GASIRIINGG QECDGK-NTA QMMARVGYYE QYCAQLVGSP 272
D.japo4      206 GATIRIINGG QECDGH-NTA QMMARVGYYQ EYCAQLVGSP 244
C.amar4      232 GSTIRAVNGG -ECGGG-NTP AVNARVGYYT QYCKQLVGSP 269
O.sat4       244 GATTRAINGA LECNGK-NPG AVNARVNYYK DYCRQFGVDP 282
```

Fig. 7. **Amino acid sequence alignment of class I and class II chitinases from plants.** Barley, a class II enzyme from *Hordeum vulgare* (*34*); Garlic1, a class I enzyme from *Allium sativum*, DDBJ Accession NO. M94105-1; Garlic2, a class I enzyme from *Allium sativum*, DDBJ Accession NO. M94106-1; kidney bean, a class I enzyme from *Phaseolus vulgaris* (*35*); yam, a class I enzyme from *Dioscorea japonica* (*36*); brassica, a class I enzyme from *Brassica napus* (*37*); populus1, a class I enzyme from *Populus trichocarpa* (*38*); populus2, a class I enzyme from *Populus trichocarpa* (*39*); zea mays1 and zea mays2, class I enzymes from *Zea mays* (*40*); RSC-a, a class I enzyme from rye seeds, *Secale cereal* (*41*); Oschia1a, a class I enzyme from rice *Oryza sativa* L. (*42*); petunia, a class II enzyme from *Petunia hybrida* (*43*); RSC-c, a class II enzyme from rye seeds, *Secale cereale* (*44*); Oschia2a, a class II enzyme from rice, *Oryza sativa* L., DDBJ Accession NO. AB016497-1; D. oppo4, a class IV chitinase from *Dioscorea oppositifolia* (gi:28268773) (*45*); D. japo4, a class IV chitinase from *Dioscorea japonica* (gi:322881); C. amar4, a class IV chitinase from *Chenopodium amaranticolor* (gi:2570160); O. sat4, a class IV chitinase from *Oryza sativa* (gi:30793457).

the calculated pK_as for Arg215 and Glu203 also suggest an interaction between these residues, consistent with the thermal unfolding data. The complete loss of enzymatic activity in R215A and E203A reveals that the interaction is important for the catalytic reaction.

Elevation of T_m upon the Addition of (GlcNAc)$_n$—In *Streptomyces* chitosanase, we have found that the transition temperature of thermal unfolding (T_m) is elevated upon the addition of oligosaccharide ligands, and that T_m elevation (ΔT_m) is enhanced as the chain length of

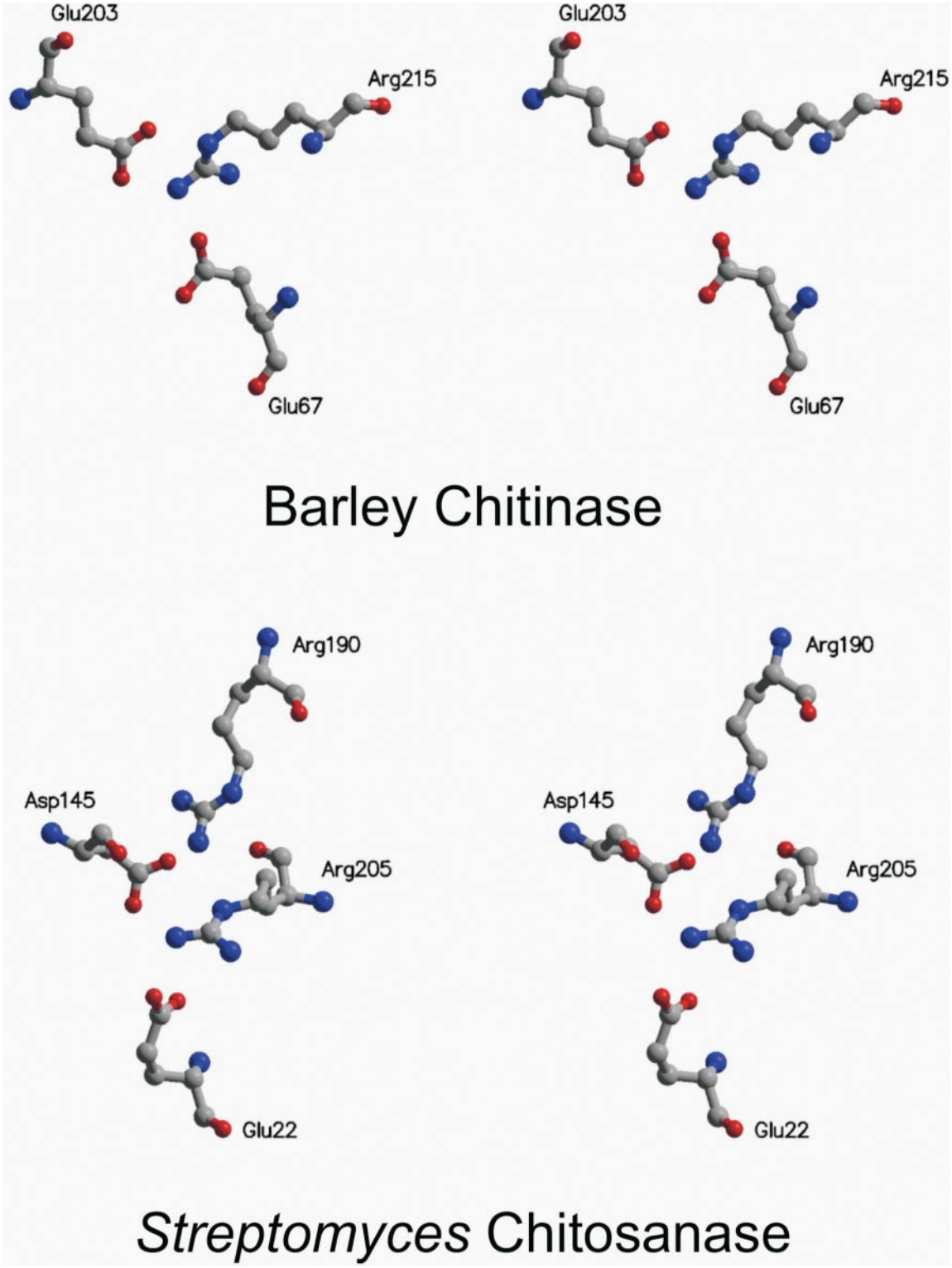

Fig. 8. **Stereo views of the interaction networks of the barley chitinase and *Streptomyces* sp. N174 chitinase**. Glu67 is the catalytic carboxylate of barley chitinase, and Glu22 is that of *Streptomyces* sp. N174 chitosanase.

the oligosaccharide added increases (*27*). To examine the substrate binding ability of the mutated chitinases, unfolding experiments were conducted in the presence of the enzyme ligands, $(GlcNAc)_n$ (n = 3 and 6). $(GlcNAc)_n$ (350-fold molar excess) was added to the enzyme solution, so that the enzyme was sufficiently saturated with ligand. Since $(GlcNAc)_n$ mixed with the enzyme solution disturbed the far UV CD spectrum, the tryptophan fluorescence intensity obtained by excitation at 295 nm was used to monitor the unfolding process. The results are shown in Fig. 6. When the inactive mutant, E67Q, was used for the experiment, the T_m value was calculated to be 53.9°C. This value is lower than that obtained by monitoring the CD at 222 nm. The CD value reflects the secondary structure of the enzyme protein, whereas the tryptophan fluorescence reflects the three-dimensional structure around the tryptophan residues. This situation seems to have resulted in the lower T_m value in the unfolding experiments based on fluorescence. The addition of $(GlcNAc)_3$ elevated the T_m value to 57.7°C (ΔT_m, 3.8°C), and the addition of $(GlcNAc)_6$ elevated it to 56.6°C (ΔT_m, 2.7°C). The ΔT_m obtained with $(GlcNAc)_6$ was unexpectedly smaller than that obtained with $(GlcNAc)_3$, suggesting that the interaction of the additional three GlcNAc residues of $(GlcNAc)_6$ with the enzyme protein might rather destabilize the enzyme structure. When E203A was used instead of E67Q, the T_m values were 48.2°C, 47.8°C [+$(GlcNAc)_3$], and 47.6°C [+$(GlcNAc)_6$]. No significant change in T_m upon the addition of saccharide ligands was found for E203A. The substrate binding ability appears to be reduced in E203A probably due to a change in local conformation at or near the catalytic center. The T_m values obtained are summarized in Table 2.

Sequence Alignment of Class I, Class II and Class IV Chitinases—Plant chitinases have been classified into at least five classes (class I to class V) based on their amino acid sequences (*28*). According to the classification of Henrissat (*5*), classes I, II, and IV belong to family GH19, while classes III and V to family GH18. Classes I and IV chitinases have a cysteine-rich domain at their N-termini, that is involved in substrate binding. The molecular sizes of class IV chitinases are smaller than those of class I chitinases due to deletions in both the cysteine-rich domain and the catalytic domain. Class II chitinases are homologous to those of classes I and IV, but do not have the cysteine-rich domain. The barley chitinase examined in this study is classified into class II. To ascertain the importance of Arg215 and Glu203, we examined the amino acid sequences of classes I, II, and IV chitinases. Figure 7 shows the sequence alignment of these classes of chitinases. Arg215 and Glu203 are completely conserved among these chitinases, indicating that they are important for enzyme function, probably due to their stabilizing effect on the catalytic cleft in all of these family GH19 chitinases.

Comparison with Other Glycosyl Hydrolases—Chitosanases hydrolyze the β-1,4-glycosidic linkage of the D-glucosamine polysaccharide, chitosan. The structure and function of the chitosanase from *Streptomyces* sp. N174, which belongs to family GH46, has been studied based on its X-ray crystal structure (*29*, *30*). Since the activities of chitinase and chitosanase are closely related to each other, these two enzymes might share a similar fold essential for catalysis. In fact, the barley chitinase and the *Streptomyces* chitosanase were found to have a structurally invariant core consisting of two α-helices and a three-stranded β-sheet, despite the fact that these enzymes share no particular sequence similarity (*4*). Similarities between these enzymes have been found as well in the subsite structure of their substrate binding cleft (*31*, *32*). In this study, we found that the barley chitinase possesses an Arg-Glu interaction essential for catalysis near the catalytic center. This interaction shows a close resemblance to an Arg-Asp-Arg interaction found in the catalytic cleft of the *Streptomyces* chitosanase, as shown in Fig. 8 (*3*). We conclude that this type of interaction network is involved in stabilizing the conformation of the catalytic cleft; hence, it is essential for catalysis in these families of glycosyl hydrolases. Another example of this type of interaction can be seen in barley 1,3-β-glucanase (*33*), which belongs to family GH17. The proton donor carboxylate of the enzyme (Glu288) is in close proximity to the ε-amino group of Lys282, which in turn is close to the Glu279 side chain. These amino acids are conserved in this family of enzymes. Analogous to the Arg–Glu interaction in the barley chitinase, the Lys282–Glu279 interaction in the barley glucanase is likely to stabilize the conformation of the catalytic cleft, and is essential for the catalytic activity.

At this stage, however, the molecular mechanism through which the cleft conformation stabilized by such a side chain interaction makes the catalytic carboxylate an efficient proton donor remains unclear. Further site-directed mutagenesis studies should be conducted using other glycosyl hydrolases, referring to the theoretical pK_a values calculated on the basis of their X-ray crystal structures. Such studies will reveal additional examples of a similar interaction network in glycosyl hydrolases.

This work was supported by a Grant-in-Aid for Exploratory Research (No. 14656043) from the Japan Society for the Promotion of Science (JSPS), 2002–2004, and in part by "Academic Frontier" Project for Private Universities: matching fund subsidy from MEXT (Ministry of Education, Culture, Sports, Science and Technology), 2004–2008. The authors are grateful to Shunji Hirose, Yumi Hayashi, Naoto Fujii, and Yoshimi Kamatsuki, Department of Food and Nutrition, Kinki University, for their technical assistance. Thanks are also due to Ms. Serena Donnini, Department of Biochemistry, University of Oulu, for her assistance in preparing the molecular models of our enzymes.

REFERENCES

1. Inoue, M., Yamada, H., Yasukochi, T., Kuroki, R., Miki, T., Horiuchi, T., and Imoto, T. (1992) Multiple role of hydrophobicity of Trp-108 in chicken lysozyme: Structural stability, saccharide binding ability, and abnormal pK_a of glutamic acid-35. *Biochemistry* **31**, 5545–5553
2. Kawaminami, S., Takahashi, H., Ito, S., Arata, Y., and Shimada, I. (1999) A multinuclear NMR study of the active site of an endoglucanase from a strain of *Bacillus*. *J. Biol. Chem.* **274**, 19823–19828
3. Fukamizo, T., Juffer, A.H., Vogel, H.J., Honda, Y., Tremblay, H., Boucher, I., Neugebauer, W.A., and Brzezinski, R. (2000) Theoretical calculation of pK_a reveals an important role of Arg205 in the activity and stability of *Streptomyces* sp. N174 chitosanase. *J. Biol. Chem.* **275**, 25633–25640
4. Monzingo, A.F., Marcotte, E.M., Hart, P.J., and Robertus, J.D. (1996) Chitinases, chitosanases, and lysozymes can be divided

into prokaryotic and eukaryotic families sharing a conserved core. *Nature Struct. Biol.* **3**, 133–140
5. Fukamizo, T (2000) Chtinolytic enzymes: Catalysis, substrate binding, and their application. *Curr. Protein Peptide Sci.* **1**, 105–124
6. Henrissat, B. (1999) Classification of chitinases modules. In *Chitin and Chitinases* (Jollès, P. and Muzzarelli, R.A.A., eds.) pp. 137–156, Birkhäuser Verlag, Basel
7. Hart, P.J., Monzingo, A.F., Ready, M.P., Ernst, S.R., and Robertus, J.D. (1995) The refined crystal structure of an endochitinase from *Hordeum vulgare* L. seeds to 1.8 Å resolution. *J. Mol. Biol.* **248**, 402–413
8. Andersen, M.D., Jensen, A., Robertus, J.D., Leah, R., and Skriver, K. (1997) Heterologous expression and characterization of wild-type and mutant forms of a 26 kDa endochitinase from barley (*Hordeum vulgare* L.). *Biochem. J.* **322**, 815–822
9. Hollis, T., Honda, Y., Fukamizo, T., Marcotte, E., Day, P.J., and Robertus, J.D. (1997) Kinetic analysis of barley chitinase. *Arch. Biochem. Biophys.* **344**, 335–342
10. Brameld, K.A. and Goddard III, W.A. (1998) The role of enzyme distortion in the single displacement mechanism of family 19 chitinases. *Proc. Natl. Acad. Sci. USA* **95**, 4276–4281
11. Brameld, K.A., Shrader, W.D., Imperiali, B., and Goddard III, W.A. (1998) Substrate assistance in the mechanism of family 18 chitinases: Theoretical studies of potential intermediates and inhibitors. *J. Mol. Biol.* **280**, 913–923
12. van Aalten, D.M.F., Komander, D., Synstad, B., Gåseidnes, S., Peter, M.G., and Eijsink, V.G.H. (2001) Structural insights into the catalytic mechanism of a family 18 exo-chitinase. *Proc Natl. Acad. Sci. USA* **98**, 8979–8984
13. Bortone, K., Monzingo, A.F., Ernst, S., and Robertus, J.D. (2002) The structure of an allosamidin complex with the *Coccidioides immitis* chitinase defines a role for a second acid residue in substrate-assisted mechanism. *J. Mol. Biol.* **320**, 293–302
14. Juffer, A.H., Argos P., and Vogel, H.J. (1997) Calculating acid-dissociation constants of proteins using the boundary element method. *J. Phys. Chem. B* **101**, 7664–7673
15. Yamada, H. and Imoto, T. (1981) A convenient synthesis of glycolchitin, a substrate of lysozyme. *Carbohydr. Res.* **92**, 160–162
16. Berman, H.M., Westbrook, J., Feng, Z., Gilliland, G., Bhat, T.N., Weissig, H., Shindyalov, I.N., and Bourne, P.E. (2000) The Protein Data Bank. *Nucleic Acids Res.* **28**, 235–242
17. Juffer, A.H., Botta, E.F.F., van Keulen, B.A.M., van der Ploeg, A., and Berendsen, H.J.C. (1991) The electric potential of a macromolecule in a solvent: A fundamental approach. *J. Comput. Phys.* **97**, 144–171
18. Juffer, A.H. (1998) Theoretical calculations of acid-dissociation constants of proteins. *Biochem. Cell Biol.* **76**, 198–209
19. Sharma, S., Pirila, P., Kaija, H., Vihko, P., and Juffer, A.H. (2005) Theoretical investigations of prostatic acid phosphatase. *Proteins* **58**, 295–308
20. Lappi, A.K., Lensink, M.F., Alanen, H.I., Salo, K.E.H., Lobell, M., Juffer, A.H., and Ruddock, L.W. (2004) A conserved arginine plays a role in the catalytic cycle of the protein disulphide isomerase. *J. Mol. Biol.* **335**, 283–295
21. Juffer, A.H. and Vogel, H.J. (2000) pK_a calculations of calbindin D9k: Effects of Ca^{2+} binding, protein dielectric constant, and ionic strength. *Proteins* **41**, 554–567
22. Imoto, T. and Yagishita, K. (1972) A simple activity measurement of lysozyme. *Agric. Biol. Chem.* **35**, 1154–1156
23. Pace, C.N., Vajdos, F., Fee, L., Grimsley, G., and Gray, T. (1995) How to measure and predict the molar absorption coefficient of a protein. *Protein Sci.* **4**, 2411–2423
24. Laemmli, U.K. (1970) Cleavage of structural proteins during the assembly of the head of bacteriophage T4. *Nature* **227**, 680–685
25. Imoto, T., Johnson, L.N., North, A.C.T., Phillips, D.C., and Rupley, J.A. (1972) Vertebrate lysozymes. In *The Enzyme*, 3rd ed., Vol. 7, Academic Press, New York
26. Joshi, M.D., Sidhu, G., Nielsen, G.E., Brayer, G.D., Withers, S.G., and McIntosh, L.P. (2001) Dissecting the electrostatic interactions and pH-dependent activity of a family 11 glycosidase. *Biochemistry* **40**, 10115–10139
27. Honda, Y., Fukamizo, T., Boucher, I., and Brzezinski, R. (1997) Substrate-binding to the inactive mutants of *Streptomyces* sp. N174 chitosanase: indirect evaluation from the thermal unfolding experiments. *FEBS Lett.* **411**, 346–350
28. Neuhaus, J.-M., Fritig, B., Linthorst, H.J.M., Meins, F., Mikkelsen, J.D., and Ryals, J. (1996) A revised nomenclature for chitinase genes. *Plant Mol. Biol. Reptr.* **14**, 102–104
29. Marcotte, E.M., Monzingo, A.F., Ernst, S.R., Brzezinski, R., and Robertus, J.D. (1996) X-ray structure of an antifungal chitosanase from *Streptomyces* N174. *Nature Struct. Biol.* **3**, 155–162
30. Fukamizo, T. and Brzezinski, R. (1997) Chitosanase from *Streptomyces* sp. strain N174: a comparative review of its structure and function. *Biochem. Cell Biol.* **75**, 687–696
31. Honda, Y. and Fukamizo, T. (1998) Substrate binding subsites of chitinase from barley seeds and lysozyme from goose egg white. *Biochim. Biophys. Acta* **1388**, 53–65
32. Tremblay, H., Yamaguchi, T., Fukamizo, T., and Brzezinski, R. (2001) Mechanism of chitosanase-oligosaccharide interaction: Subsite structure of *Streptomyces* sp. N174 chitosanase and the role of Asp57 carboxylate, *J. Biochem.* **130**, 679–686
33. Chen, L., Garrett, T.P.J., Fincher, G.B., and Høj, P.B. (1995) A tetrad of ionizable amino acids is important for catalysis in barley β-glucanases. *J. Biol. Chem.* **270**, 8093–8101
34. Leah, R., Tommerup, H., Svendsen, I., and Mundy, J. (1991) Biochemical and molecular characterization of three barley seed proteins with antifungal properties. *J. Biol. Chem.* **266**, 1564–1573
35. Broglie, K.E., Gaynor, J.J., and Broglie, R.M. (1986) Ethylene-regulated gene expression: molecular cloning of the genes encoding an endochitinase from *Phaseolus vulgaris*. *Proc. Natl. Acad. Sci. USA* **83**, 6820–6824
36. Araki, T., Funatsu, J., Kuramoto, M., Konno, H., and Torikata, T. (1992) The complete amino acid sequence of yam (*Dioscorea japonica*) chitinase. A newly identified acidic class I chitinase. *J. Biol. Chem.* **267**, 19944–19947
37. Rasmussen, U., Bojsen, K., and Collinge, D.B. (1992) Cloning and characterization of a pathogen-induced chitinase in *Brassica napus*. *Plant Mol. Biol.* **20**, 277–287
38. Parsons, T.J., Bradshaw, H.D. Jr., and Gordon, M.P. (1989) Systemic accumulation of specific mRNAs in response to wounding in poplar trees. *Proc. Natl. Acad. Sci. USA* **86**, 7895–7899
39. Davis, J.M., Clarke, H.R., Bradshaw, H.D. Jr., and Gordon, M.P. (1991) *Populus* chitinase gene: structure, organization, and similarity of translated sequences to herbaceous plant chitinases. *Plant Mol. Biol.* **17**, 631–639
40. Huynh, Q.K., Hironaka, C.M., Levine, E.B., Smith, C.E., Borgmeyer, J.R., and Shah, D.M. (1992) Antifungal proteins from plants: Purification, molecular cloning, and antifungal properties of chitinases from maize seed. *J. Biol. Chem.* **267**, 6635–6640
41. Yamagami, T. and Funatsu, G. (1994) The complete amino acid sequence of chitinase-a from the seeds of rye (*Secale cereal*). *Biosci Biotechnol Biochem.* **58**, 322–329
42. Nishizawa, Y., Kishimoto, N., Saito, A., and Hibi, T. (1993) Sequence variation, differential expression and chromosomal location of rice chitinase genes. *Mol. Gen. Genet.* **241**, 1–10

43. Linthorst, H.J., van Loon, L.C., van Rossum, C.M., Mayer, A., Bol, J.F., van Roekel, J.S., Meulenhoff, E.J., and Cornelissen, B.J. (1990) Analysis of acidic and basic chitinases from tobacco and petunia and their constitutive expression in transgenic tobacco. *Mol. Plant Microb. Interact.* **3**, 252–258
44. Ohnuma, T., Yagi, M., Yamagami, T., Taira, T., Aso, Y., and Ishiguro, M. (2002) Molecular cloning, functional expression, and mutagenesis of cDNA encoding rye (*Secale cereale*) seed chitinase-c. *Biosci. Biotechnol. Biochem.* **66**, 277–284
45. Mitsunaga, T., Iwase, M., Ubhayasekera, W., Mowbray, S.L., and Koga, D. (2004) Molecular cloning of a genomic DNA encoding yam class IV chitinase. *Biosci. Biotechnol. Biochem.* **68**, 1508–1517